

**DYNAMICAL PLANE STRUCTURES IN THE PARAMETER PLANE
OF COSINE-ROOT FAMILY**

HONORS THESIS
ITHACA COLLEGE

DEPARTMENT OF MATHEMATICS

BY
MAKSIM SIPOS

FACULTY MENTOR: DAVID BROWN

ITHACA, NY
MAY 2007

ABSTRACT

We analyze the existence of structures in the parameter plane of the family of functions of the form $\alpha \cos \sqrt{z}$. These structures look like certain Julia sets of the quadratic polynomials.

TABLE OF CONTENTS

ABSTRACT		ii
LIST OF FIGURES		iv
LIST OF TABLES		v
1	INTRODUCTION	1
1.1	Dynamical Systems	1
1.2	Chaotic Orbits	2
1.3	Complex Dynamics	3
1.4	$z^2 + c$ Family	4
1.5	Mandelbrot Set	5
1.6	Cosine-Root Family	7
2	EXPERIMENTAL RESULTS	11
2.1	Dynamical Plane Features	11
2.2	Mapping from the Cosine-Root Parameter Plane to the Mandelbrot Set	13
2.3	Second Iterate of $-\alpha$	15
2.4	$g(\alpha)$ Locating the B_n	19
3	ANALYTICAL RESULTS	20
3.1	$g(\alpha)$ Locate the B_n	20
3.2	The Immediate Basin of Attraction	22

LIST OF FIGURES

1.1	An example of the filled Julia set of Q_c	6
1.2	The Mandelbrot set.	8
1.3	An example Julia set for C_α . For more clarity, the shading was made to show the rate of points' escape outside of the bounding parabolas. All points that aren't white are in the Julia set for this value of α	9
1.4	An overview of the parameter plane of C_α	10
2.1	The region of the parameter plane where the Julia-like structures appear.	12
2.2	One of the top-level Julia-like structures in the large green cardioid.	13
2.3	These Julia-like structures exist in the green cardioid and do not intersect the real axis.	15
2.4	The left side indicates the images of the Julia-like structures in the cosine-root family parameter plane. The right side indicates the images of $K_{m(z_0)}$ where z_0 is the empirically-estimated center of the corresponding Julia-like structure and function $m(z)$ is defined by (2.2).	16
2.5	An example of a plot of the immediate basin of attraction. The X-s indicate the values of the second, third, and fourth iterates of $-\alpha$. The star indicates the attracting fixed point for this α . It is apparent from this figure that the second, third and fourth iterates of $-\alpha$ lie inside the immediate basin of attraction.	18
2.6	The plot of $g(\alpha)$ for $\alpha \in [37.5, 41.5]$. The shaded regions indicate the α inside the first four Julia-like structures (B_1 through B_4). The shapes of the B_n are indicated by arrows.	19

LIST OF TABLES

1.1	Coloring of the parameter-plane images of C_α	10
2.1	Empirically-found locations of the large Julia-like structures. The two columns indicate the left and right edges of the structure along the real line.	14
2.2	Some iterations of $-\alpha$ when $\alpha \in B_2$. $w_\alpha = \lim_{n \rightarrow \infty} C_\alpha^n(-\alpha)$, that is, w_α is the attracting fixed point of C_α	17

CHAPTER 1

INTRODUCTION

1.1 Dynamical Systems

The goal of our study is to understand the asymptotic behaviour of points in a dynamical process. Let S be a set and let $f : S \rightarrow S$ be a function. We are interested in a discrete process, the iteration of f , and hope to understand the eventual behavior of the points $x, f(x), f^2(x), f^3(x), \dots$.

Definition 1.1.1. *The forward orbit of x under f is the sequence*

$$O^+(x) = \{x, f(x), f^2(x), f^3(x), \dots\}. \quad (1.1)$$

Certain points may have important, and easy-to-describe behaviour under a mapping.

Definition 1.1.2. *A point x is a **fixed point** for f if $f(x) = x$.*

Definition 1.1.3. *A point x is a **periodic point** for f of period n if $f^n(x) = x$. The least positive integer n for which $f^n(x) = x$ is called the **prime period** of x .*

It follows that, if x is a periodic point of prime period n , then x is a fixed point of the function f^n .

If f is differentiable at a fixed point x , then $f'(x)$ yields information about the forward orbits of points around x .

Definition 1.1.4. If $f(x) = x$ and $|f'(x)| < 1$, then x is an **attracting fixed point**. That is, there exists an open interval I around x such that $f(I) \subset I$.

Definition 1.1.5. If $f(x) = x$ and $f'(x) = 0$, then we call x a **superattracting fixed point**.

1.2 Chaotic Orbits

Let $f : \mathbb{C} \rightarrow \mathbb{C}$ be a continuous function. We will define what we mean by saying that an orbit under f is chaotic.

Definition 1.2.1. f is said to be **topologically transitive** on S if, for any pair of open sets $U, V \subset S$, there exists k such that $f^k(U) \cap V \neq \emptyset$.

Intuitively, a map that is topologically transitive allows one to reach any arbitrarily small neighborhood in S from any other such neighborhood in S in a certain number of iterations. That is, S is not split into two disjoint subsets where it is impossible to map from one to another in any finite number of iterations.

Definition 1.2.2. f has **sensitive dependence on initial conditions** if there exists $\delta > 0$ such that, for any $z \in S$, and any neighborhood V of z , there exists $w \in V$ and $n \geq 0$ such that $|f^n(z) - f^n(w)| > \delta$.

Intuitively, a function that has sensitive dependence on initial conditions will separate a point arbitrarily close to z from z by at least δ , after n iterations. Not all points near z need be separated like that. But there must exist at least one such point in every neighborhood of z .

Definition 1.2.3. A subset A of S is **dense** in S , if for any point $z \in S$, every neighborhood of z contains at least one point in A .

Definition 1.2.4. f is said to be **chaotic** on S if

1. f has sensitive dependence on initial conditions,
2. f is topologically transitive,
3. f set of periodic points of f is dense in S .

Intuitively, chaotic orbits have elements of unpredictability (because of the sensitive dependence), indecomposability (because of topological transitivity) but also regularity (since the periodic points are dense).

1.3 Complex Dynamics

The behavior of maps of the complex plane can be further investigated by looking at the effects of attracting fixed points.

Definition 1.3.1. The family $\{F_n\}$ of functions is a **normal family** on U if every sequence of the F_n 's has a subsequence which either

1. converges uniformly on compact subsets of U , or
2. converges uniformly to ∞ on U .

Example 1.3.2. Let $F(z) = az$ where $|a| > 1$. Let F_n be the n^{th} iterate of F . Then, $\{F_n\}$ is a normal family on every domain of \mathbb{C} that does not include 0.

If the mapping is a normal family on a domain of \mathbb{C} , then the orbits of points in that domain are similar to those of nearby points.

Definition 1.3.3. The **Fatou set** (also called the normal set, or stable set) of f , is the subset of \mathbb{C} on which $\{f^n\}$ is a normal family.

If f is a polynomial function, then all orbits of z in the Fatou set will either diverge to infinity or be attracted to a fixed point or a cycle. Considering ∞ as a point on the Riemann sphere, we see that, for a polynomial, this point would act as an attractor.

Definition 1.3.4. *The **Julia set** of f , denoted J_f , is the complement of the Fatou set.*

As opposed to the tame dynamics on the Fatou set, the dynamics on the Julia set are chaotic.

The orbits of certain points give important information about the topology of the Julia set.

Definition 1.3.5. *Let $f : \mathbb{C} \rightarrow \mathbb{C}$ be an analytic function. Then z is a critical point of f if $f'(z) = 0$.*

1.4 $z^2 + c$ Family

Now, let us consider a family of parametrized functions of the form

$$Q_c(z) = z^2 + c \tag{1.2}$$

where $c \in \mathbb{C}$. Some special results hold for this family (and in fact, for the general family of polynomial functions).

Definition 1.4.1. *The **filled Julia set** of a polynomial f , denoted K_f , is the set of all points with bounded orbits under f .*

Theorem 1.4.2. *The boundary of K_f is J_f .*

Proof. See [1].

□

Example 1.4.3. Given the definition and the theorem, we see that the Julia set of Q_0 is the unit circle $\{z : |z| = 1\}$.

Theorem 1.4.4. Let $z \in \mathbb{C}$ and $|z| > 2$. Then, for any $c \in \mathbb{C}$, $Q_c^n(z) \rightarrow \infty$ as $n \rightarrow \infty$.

Proof. See [1]. □

This gives us a way to visualize filled Julia sets of $z^2 + c$:

1. Let z be a point in the window of the complex plane we are visualizing.
2. Iterate Q_c starting at z , to generate the set of points $S = \{Q_c(z), Q_c^2(z), \dots, Q_c^n(z)\}$.
 $n \in \mathbb{N}$ is the maximum number of iterations we want.
3. If, for any $z_0 \in S$, we have $|z_0| > 2$, then color that point white (its orbit is unbounded and it does not belong to the filled Julia set). Otherwise, color the point black.

Of course, Theorem 1.4.4 also lets us stop the iterations as soon as any iteration leads to a point whose absolute value is greater than 2.

Figure 1.1 shows an example of a filled Julia set of Q_c . It must be noted that these images of the Julia sets are only approximations drawn using finite-precision numerical computation.

1.5 Mandelbrot Set

As noted in Section 1.3, the orbits of critical points are especially important. For Q_c , the only critical point is 0. Fatou proved the following result ([1]).

Theorem 1.5.1. If $Q_c^n(0) \not\rightarrow \infty$, then K_{Q_c} is connected.

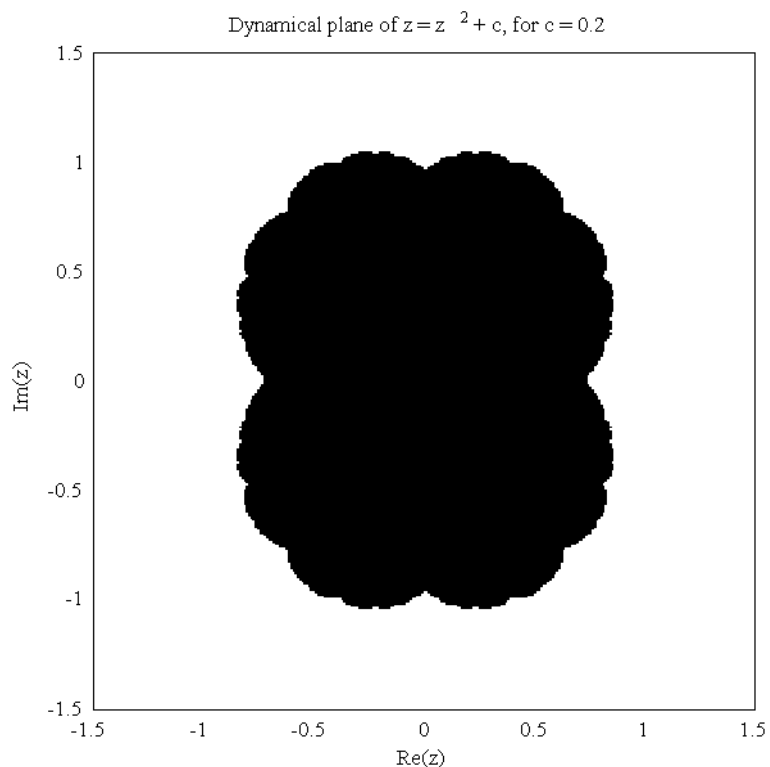


Figure 1.1: An example of the filled Julia set of Q_c .

We can define a set of points c for which K_{Q_c} is connected; this set is called the **Mandelbrot set**. By Theorem 1.5.1, we have

Corollary 1.5.2. *The Mandelbrot set is the subset of the c -plane given by*

$$\mathcal{M} = \{c : Q_c^n(0) \not\rightarrow \infty\}. \quad (1.3)$$

The following theorem shows the Mandelbrot set is limited to the points $\{z : |z| \leq 2\}$.

Theorem 1.5.3. *Let $z \in \mathbb{C}$ and $|c| > 2$. Then, $Q_c^n(z) \rightarrow \infty$ as $n \rightarrow \infty$.*

Proof. See [1].

□

The Mandelbrot set is visualized in a way analogous to the Julia set:

1. Let z be a point in the window of the complex plane we are visualizing.
2. Iterate Q_c starting at 0, to generate the set of points $S = \{Q_c(0), Q_c^2(0), \dots, Q_c^n(0)\}$.
 $n \in \mathbb{N}$ is the maximum number of iterations we want.
3. If, for any $z_0 \in S$, we have $|z_0| > 2$, then color that point white (it's orbit is unbounded and it does not belong to the Mandelbrot set). Otherwise, color the point black.

The Mandelbrot set is visualized in Figure 1.2. The cusp of the large cardioid is located at $1/4$. The left-most point of the cardioid is at $-3/4$. The largest bulb attached to the Cardioid is of radius $1/4$ centered at -1 .

1.6 Cosine-Root Family

We consider the parametrized function

$$C_\alpha(z) = \alpha \cos \sqrt{z}, \tag{1.4}$$

where $\alpha \in \mathbb{C}$. This function is a transcendental function, and Picard's Theorem states that any neighborhood U of infinity on the Riemann sphere (that is, the set $U = \{z : |z| > r\}$, $r \in \mathbb{R}$) gets mapped across the whole plane (with the exception of at most one point), in a single iteration. This is very different from polynomials such as Q_c , where ∞ acts like an attracting fixed point.

Thus, for transcendental functions, the points with unbounded orbits are not in the Fatou set, and hence lie in the Julia set.

Theorem 1.6.1. *The set of points whose orbits are unbounded lie in J_{C_α} .*

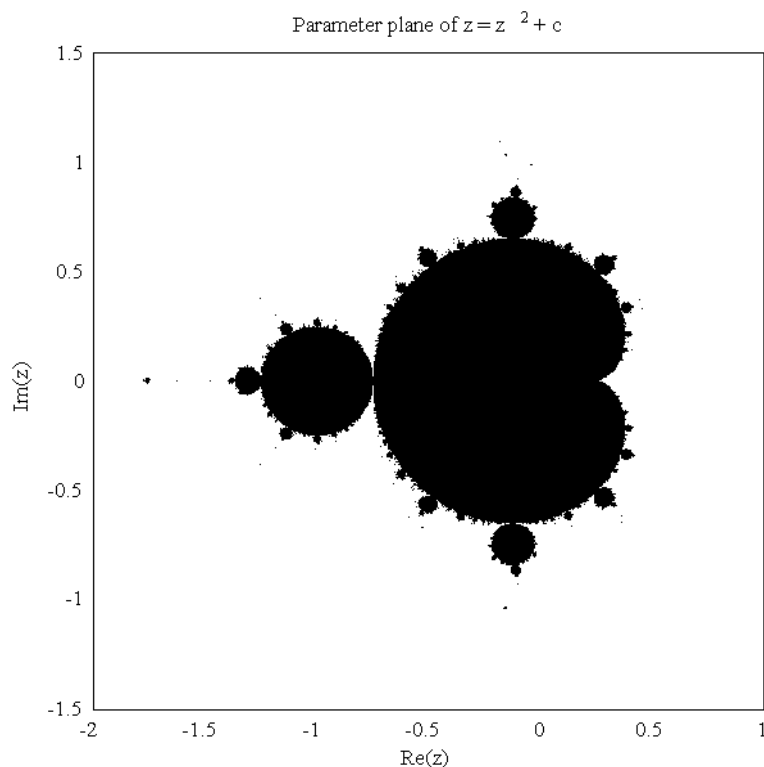


Figure 1.2: The Mandelbrot set.

The visualization of Julia sets for C_α is performed in the same way as described in Section 1.4. Note, however, that this time, the black points (indicating the points inside the Julia set) are the ones whose orbits are unbounded. Also, the criterion in Theorem 1.4.4 becomes the following [2].

Theorem 1.6.2. *A point z is in J_{C_α} if*

$$|\operatorname{Im}(\sqrt{z})| > 50 \tag{1.5}$$

which is equivalent to

$$\operatorname{Re}(z) \geq \frac{(\operatorname{Im}(z))^2}{10,000} - 2,500. \tag{1.6}$$

Proof. See [2]. □

An example of a visualization of a Julia set for C_α is given in Figure 1.3.

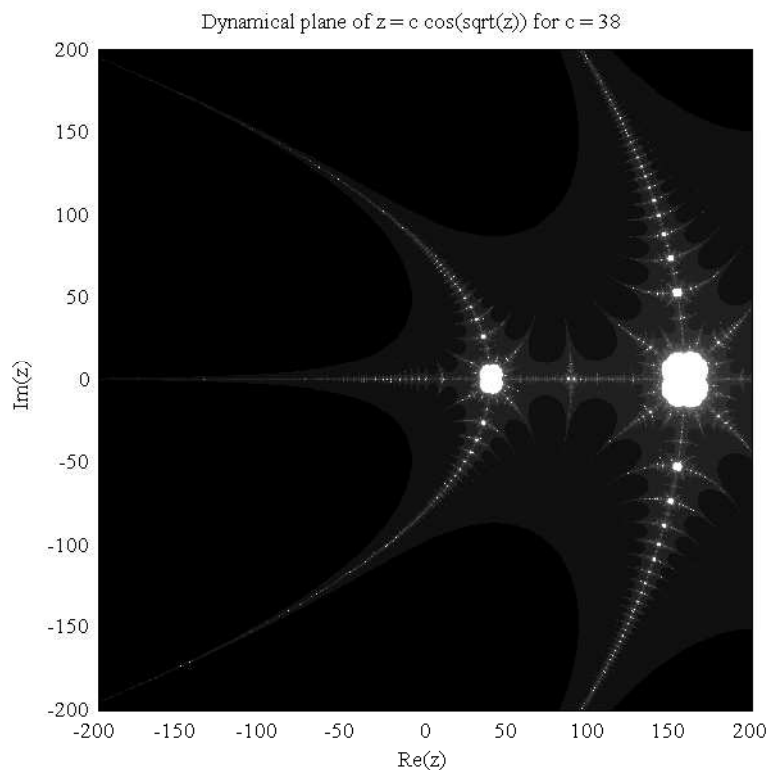


Figure 1.3: An example Julia set for C_α . For more clarity, the shading was made to show the rate of points' escape outside of the bounding parabolas. All points that aren't white are in the Julia set for this value of α .

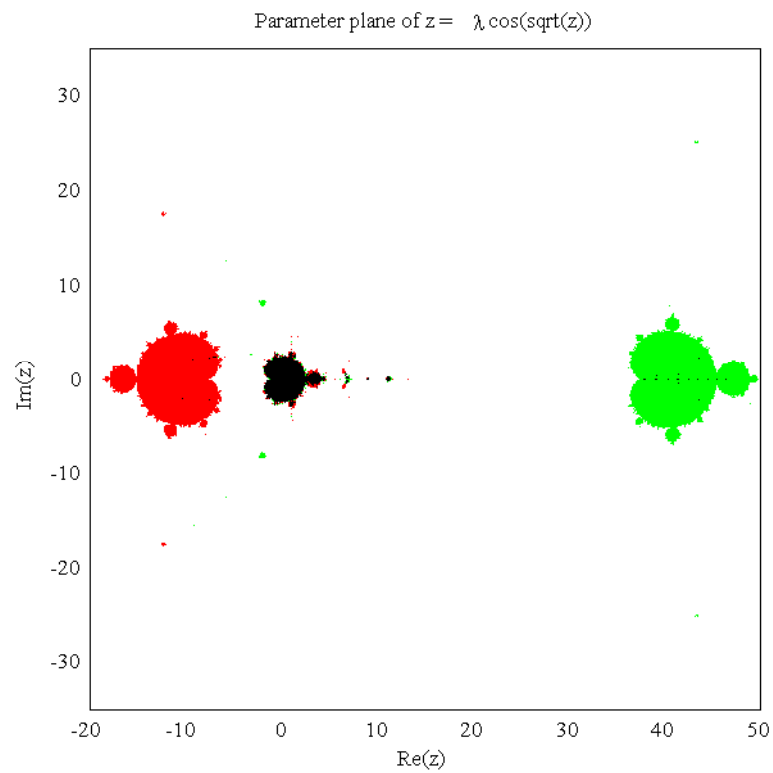
Similar to our analysis of the Mandelbrot set, we can analyze the parameter plane of C_α . C_α has infinitely many critical points given by $n^2\pi^2$, where $n \in \mathbb{N}$. However, the orbits of the critical points lead to only two distinct critical values $\pm\alpha$.

We generate the parameter plane images by using 4 colors, specifying all possible combinations of boundedness (or unboundedness) of critical values. The meanings of the colors are given in Table 1.1.

An overview of the parameter plane of C_α is shown in Figure 1.4.

Table 1.1: Coloring of the parameter-plane images of C_α .

Critical Value Orbit	α escapes	α bounded
$-\alpha$ escapes	White	Green
$-\alpha$ bounded	Red	Black

Figure 1.4: An overview of the parameter plane of C_α .

CHAPTER 2

EXPERIMENTAL RESULTS

2.1 Dynamical Plane Features

When observing the parameter plane of the cosine-root family of transcendental functions, we interestingly note the appearance of Julia-like structures from the $z^2 + c$ family. One does not expect such behavior in the parameter plane. The Julia-like structures appear in the parameter plane in the window given in Figure 2.1.

In particular our analysis will focus on the top-level Julia-like structures in the large green cardioid. By top-level we mean the following. There seems to be infinitely many Julia-like structures in the green cardioid. In a fractal-like manner, their sizes vary. By top-level structures, we mean those whose area is the largest. An example of a top-level Julia-like structure is shown in Figure 2.2.

There are seven such top-level structures in the green cardioid, and name them B_1 through B_7 (in order of increasing real values of their position). Empirically, we found that the green cardioid's intersection with the real line is the interval $[37.46095 \pm 0.0001, 45.23 \pm 0.01]$. Also empirically, we have found the locations of B_n by plotting the parameter planes with increasing numbers of iterations and greater resolutions. They are shown in Table 2.1. We found that these structure locations were of importance to our conjectures. In fact, we have evidence to believe that the B_n are values for which the second iterate of $-\alpha$ lies in the immediate basin of attraction of the attracting fixed point of C_α .

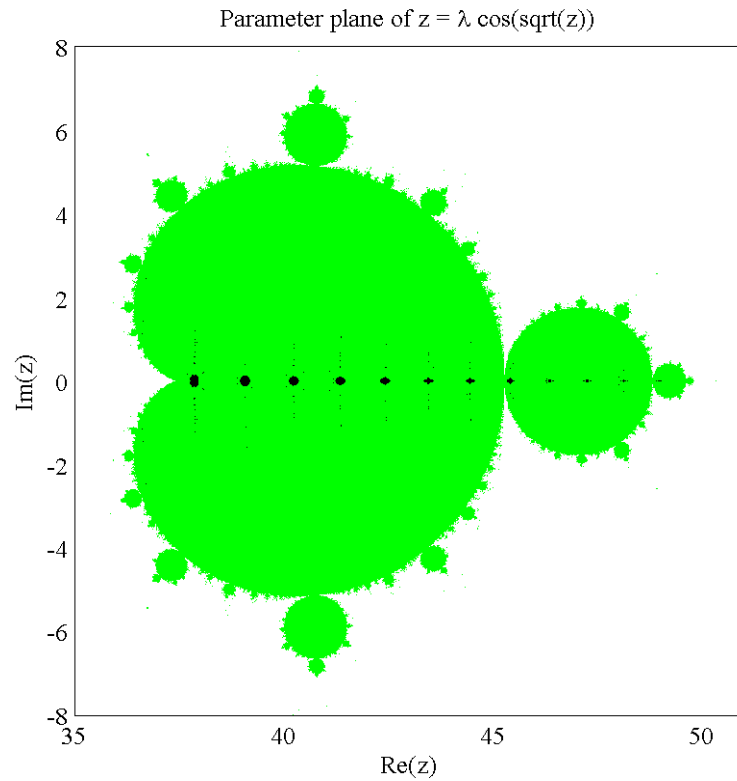


Figure 2.1: The region of the parameter plane where the Julia-like structures appear.

We have limited our analysis to the Julia-like structures along the real line and the dynamics along the real line. However, it is important to note that such Julia-like structures (of small size, compared to the B_n) exist in the cardioid that do not intersect the real axis, “sprouting” up and down from the real axis. See Figure 2.3 as an example.

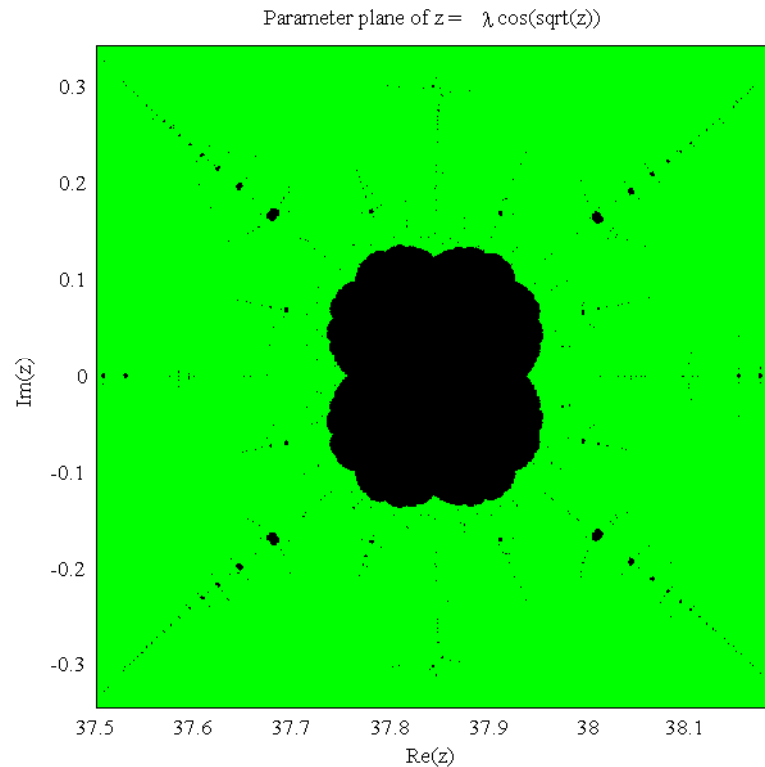


Figure 2.2: One of the top-level Julia-like structures in the large green cardioid.

2.2 Mapping from the Cosine-Root Parameter Plane to the Mandelbrot Set

As shown in Figure 2.1, the Julia-like structures exist in a green region in the shape of a Mandelbrot set. Thus, we can create a function $m : \mathbb{C} \rightarrow \mathbb{C}$ from the cosine-root parameter plane to that of the Mandelbrot set. We can use the two points described in Section 2.1, the endpoints of the intersection of the green cardioid, to define our two-dimensional transformation. Under our transformation, we expect m to map the cusp of the green shape to that of the Mandelbrot set cardioid (see Section 1.5). Similarly, we expect m to map the right-most point of the cardioid to the corresponding one in

Table 2.1: Empirically-found locations of the large Julia-like structures. The two columns indicate the left and right edges of the structure along the real line.

	Left Edge	Right Edge
B_1 :	37.75 ± 0.01	37.935 ± 0.01
B_2 :	38.943 ± 0.005	39.166 ± 0.005
B_3 :	40.091 ± 0.005	40.333 ± 0.005
B_4 :	41.197 ± 0.005	41.449 ± 0.005
B_5 :	42.263 ± 0.005	42.5205 ± 0.0005
B_6 :	43.291 ± 0.001	43.551 ± 0.001
B_7 :	44.284 ± 0.001	44.545 ± 0.001

the Mandelbrot set. That is,

$$m(37.46095) = \frac{1}{4} \quad \text{and} \quad m(45.23) = -\frac{3}{4}. \quad (2.1)$$

Looking at Figure 2.1, we expect this transformation to be linear. This is because the green region in the shape of a Mandelbrot set does not seem skewed or stretched in any nonlinear way. Thus, supposing $m(z) = az + b$ and using (2.1) yields

$$m(z) = -0.1287z + 5.0718. \quad (2.2)$$

We can proceed to test our mapping $m(z)$ by comparing the images of the Julia-like structures centered at z_0 with the actual quadratic filled Julia sets $K_{m(z_0)}$. This comparison is shown in Figure 2.4. Note that the comparison shows correlation to the quadratic Julia sets, even for those Julia-like structures that are not along the real axis. Interestingly, we also find that certain Julia-like structures are rotated.

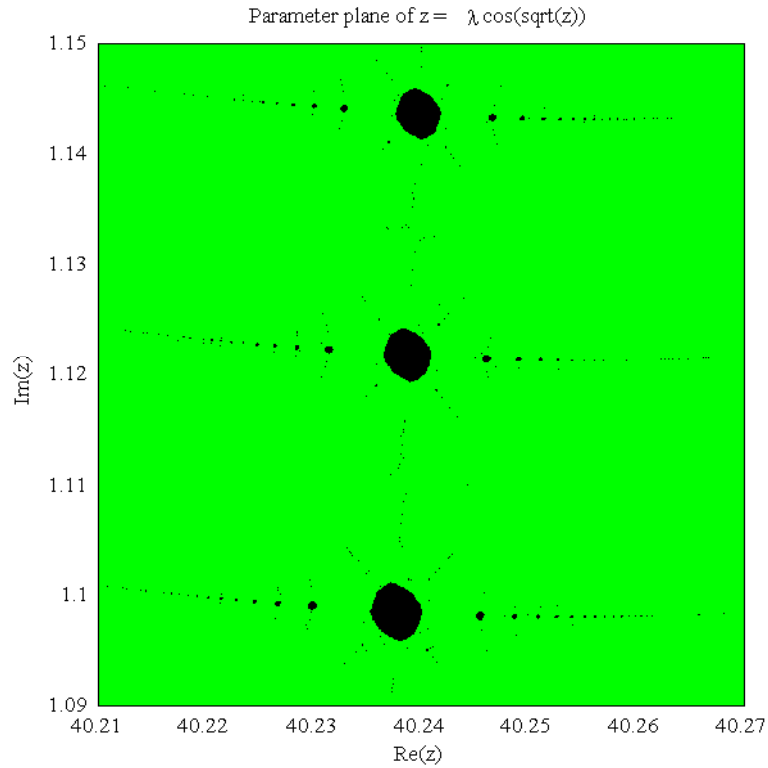


Figure 2.3: These Julia-like structures exist in the green cardioid and do not intersect the real axis.

2.3 Second Iterate of $-\alpha$

Inside the green cardioid, the orbit of critical value α is always bounded. However, the orbit of $-\alpha$ may be bounded or unbounded, depending on α . When it is bounded, we are inside a Julia-like structure. Thus, we considered the iterations of $-\alpha$, along the intersection of the large Julia-like structures. Along the real line, the function C_α becomes:

$$C_\alpha(x) = \begin{cases} \alpha \cos \sqrt{x} & \text{if } x > 0; \\ \alpha \cosh \sqrt{|x|} & \text{if } x < 0. \end{cases} \quad (2.3)$$

In particular, we found interesting the behaviour of the iterates of $-\alpha$. Table 2.2 shows an example of such iterations. In particular if we plot the Julia set of C_α , for

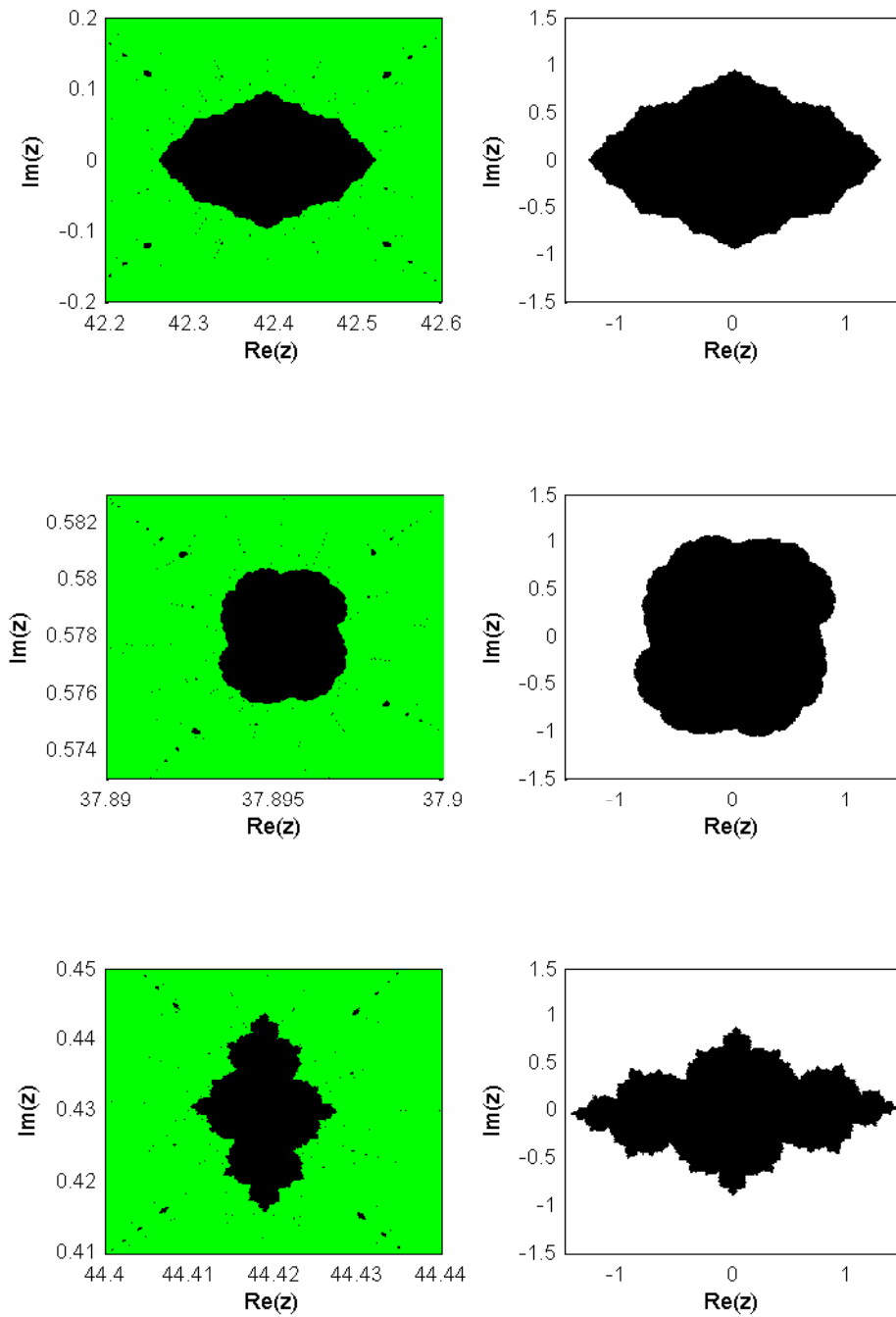


Figure 2.4: The left side indicates the images of the Julia-like structures in the cosine-root family parameter plane. The right side indicates the images of $K_{m(z_0)}$ where z_0 is the empirically-estimated center of the corresponding Julia-like structure and function $m(z)$ is defined by (2.2). Note the rotation of the Julia-like structures we didn't expect.

Table 2.2: Some iterations of $-\alpha$ when $\alpha \in B_2$. $w_\alpha = \lim_{n \rightarrow \infty} C_\alpha^n(-\alpha)$, that is, w_α is the attracting fixed point of C_α .

α	C_α -iterates of $-\alpha$	w_α
38.945	$-38.945 \rightarrow 9992.598 \rightarrow 32.830 \rightarrow 33.132 \rightarrow 33.658 \rightarrow \dots$	38.904
38.983	$-38.983 \rightarrow 10032.584 \rightarrow 36.370 \rightarrow 37.747 \rightarrow 38.605 \rightarrow \dots$	38.948
39.028	$-39.028 \rightarrow 10080.746 \rightarrow 38.709 \rightarrow 38.954 \rightarrow 38.993 \rightarrow \dots$	39.000
39.066	$-39.066 \rightarrow 10121.031 \rightarrow 38.964 \rightarrow 39.033 \rightarrow 39.041 \rightarrow \dots$	39.042
39.104	$-39.104 \rightarrow 10161.453 \rightarrow 37.655 \rightarrow 38.683 \rightarrow 39.024 \rightarrow \dots$	39.084
39.149	$-39.149 \rightarrow 10210.140 \rightarrow 34.085 \rightarrow 35.337 \rightarrow 36.924 \rightarrow \dots$	39.134

each of the orbits shown in Table 2.2, we find that the second iterate of $-\alpha$ always lies within the immediate basin of attraction of the attracting fixed point. An example of such a plot is shown in Figure 2.5. The first iterate of $-\alpha$, when $\alpha > 0$, is

$$C_\alpha(-\alpha) = \alpha \cosh \sqrt{\alpha}.$$

Hyperbolic cosine is always positive, thus we define the second iterate of $-\alpha$ as the function

$$g(\alpha) = C_\alpha(C_\alpha(-\alpha)) = \alpha \cos \sqrt{\alpha \cosh \sqrt{\alpha}}.$$

The results shown in Table 2.2 and Figure 2.5 motivate the following conjecture.

Conjecture 2.3.1. *If $\alpha \in B_n$, then $g(\alpha)$ lies within the immediate basin of attraction of the attracting fixed point q_α of C_α .*

Thus, we suspect that $-\alpha$ reaches the immediate basin of attraction of q_α in two iterations. Some steps towards proving this conjecture are given in Section 3.2.

The number of iterations it takes $-\alpha$ to reach the immediate basin of attraction of q_α is important, because a point cannot leave the basin of attraction.

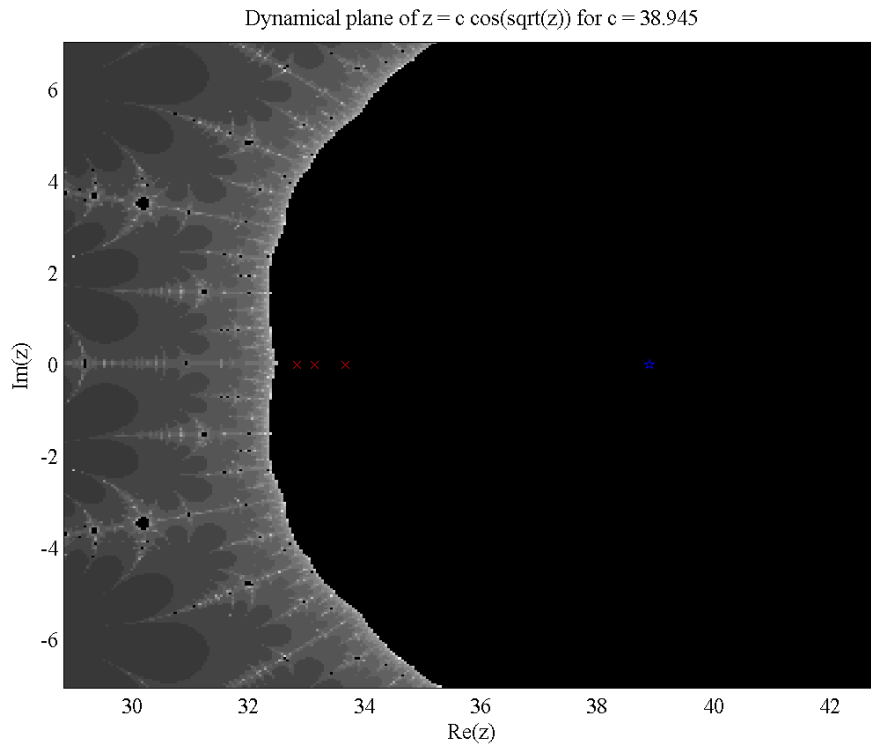


Figure 2.5: An example of a plot of the immediate basin of attraction. The X-s indicate the values of the second, third, and fourth iterates of $-\alpha$. The star indicates the attracting fixed point for this α . It is apparent from this figure that the second, third and fourth iterates of $-\alpha$ lie inside the immediate basin of attraction.

Theorem 2.3.2 (Koenig's Theorem). *Let q be the attracting fixed point of $f(z)$ and let $a = f'(q)$. If $0 < |a| < 1$, then there exists a holomorphic map $w = \phi(z)$ with $\phi(0) = 0$ so that $\phi \circ f \circ \phi^{-1}$ is the linear map $w \rightarrow aw$ for all w in some neighborhood of the origin.*

Furthemore, the basin of attraction of q_α is simply connected. Therefore, by Koenig's Theorem, inside the basin of attraction, any orbit approaches q_α .

2.4 $g(\alpha)$ Locating the B_n

We found a correlation between the values of $g(\alpha)$ and the locations of B_n , along the real line. In particular, we found that the B_n are located at the points for which $g(\alpha)$ is near a local maximum. Our results are best shown visually, as in Figure 2.6.

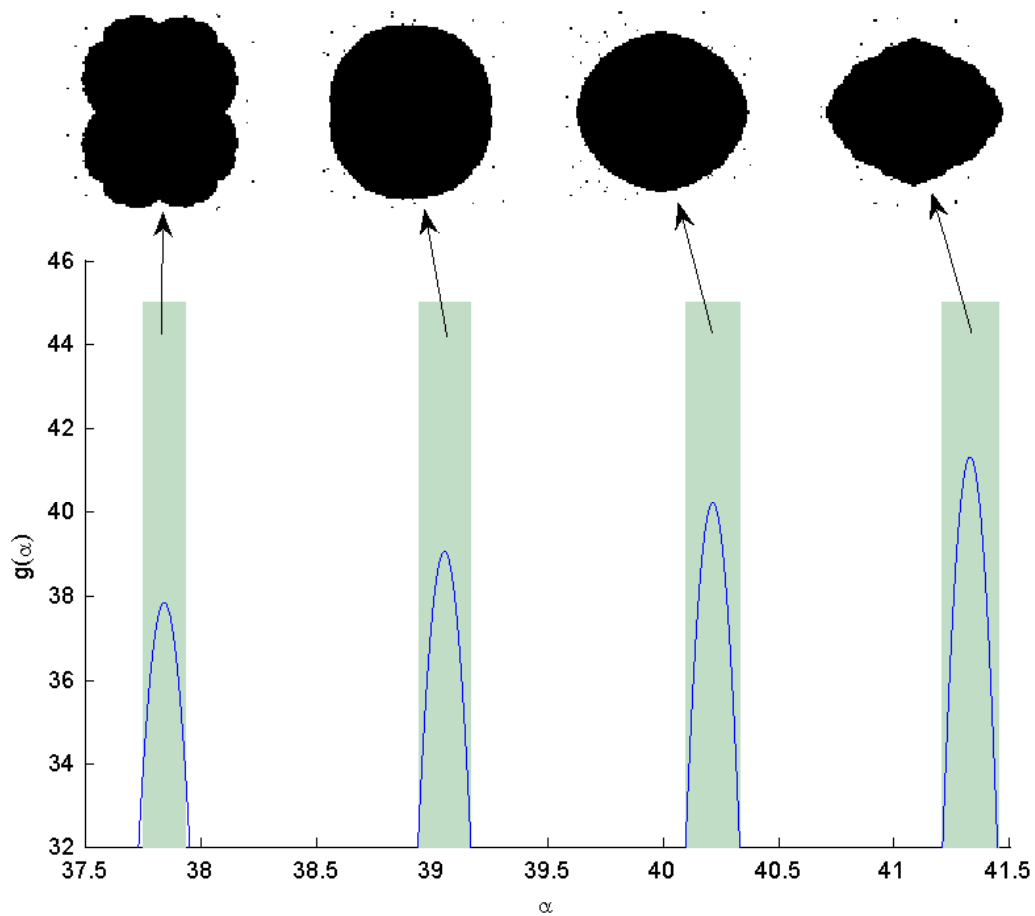


Figure 2.6: The plot of $g(\alpha)$ for $\alpha \in [37.5, 41.5]$. The shaded regions indicate the α inside the first four Julia-like structures (B_1 through B_4). The shapes of the B_n are indicated by arrows.

CHAPTER 3

ANALYTICAL RESULTS

3.1 $g(\alpha)$ Locate the B_n

The second iterate of $-\alpha$ along the real line, is the function

$$g(\alpha) = \alpha \cos \sqrt{\alpha \cosh \sqrt{\alpha}}. \quad (3.1)$$

Lemma 3.1.1. *If $g(\alpha) = \alpha$ then $g'(\alpha) = 1$.*

Proof. We have,

$$g'(\alpha) = -\alpha \sin \sqrt{\alpha \cosh \sqrt{\alpha}} \frac{d}{d\alpha} \left(\sqrt{\alpha \cosh \sqrt{\alpha}} \right) + \cos \sqrt{\alpha \cosh \sqrt{\alpha}}.$$

Furthermore,

$$\begin{aligned} \frac{d}{d\alpha} \left(\sqrt{\alpha \cosh \sqrt{\alpha}} \right) &= \frac{1}{2\sqrt{\alpha \cosh \sqrt{\alpha}}} \frac{d}{d\alpha} (\alpha \cosh \sqrt{\alpha}) \\ &= \frac{1}{2\sqrt{\alpha \cosh \sqrt{\alpha}}} \left[\cosh \sqrt{\alpha} + \frac{\alpha \sinh \sqrt{\alpha}}{2\sqrt{\alpha}} \right]. \end{aligned}$$

Thus,

$$g'(\alpha) = -\frac{\alpha \sin \sqrt{\alpha \cosh \sqrt{\alpha}}}{2\sqrt{\alpha \cosh \sqrt{\alpha}}} \left[\cosh \sqrt{\alpha} + \frac{\alpha \sinh \sqrt{\alpha}}{2\sqrt{\alpha}} \right] + \cos \sqrt{\alpha \cosh \sqrt{\alpha}} \quad (3.2)$$

If a point satisfies $g(\alpha) = \alpha$, then

$$\alpha \cos \sqrt{\alpha \cosh \sqrt{\alpha}} = \alpha, \quad (3.3)$$

$$\sqrt{\alpha \cosh \sqrt{\alpha}} = 2n\pi, \quad (3.4)$$

where $n \in \mathbb{N}$. Substituting into (3.2):

$$\begin{aligned} g'(\alpha) &= -\frac{\alpha \sin(2n\pi)}{2(2n\pi)} \left[\cosh \sqrt{\alpha} + \frac{\alpha \sinh \sqrt{\alpha}}{2\sqrt{\alpha}} \right] + \cos(2n\pi) \\ &= 1. \end{aligned}$$

□

It is of interest to qualitatively describe what happens when $g(\alpha) = \alpha$. In those cases, the second iterate of one critical value, $-\alpha$, is the second critical value α . We say that $-\alpha$ is “captured” by the orbit of α . At these points the graph of $g(\alpha)$ meets tangentially to the graph $y(\alpha) = \alpha$.

Theorem 3.1.2 (Location Theorem). *There are exactly 7 α -values in the interval $[37.46095, 45.23]$, corresponding to the green Mandelbrot, for which $g(\alpha) = \alpha$, and $g'(\alpha) = 1$.*

Proof. By (3.3) if $g(\alpha) = \alpha$, then

$$\alpha \cosh \sqrt{\alpha} = 4n^2\pi^2, \quad (3.5)$$

the left side of which is a monotonically increasing, continuous, function of α , for $\alpha > 0$. If $\alpha = 37.46095$,

$$\text{Left side} = 8524.433.$$

If $\alpha = 45.23$

$$\text{Left side} = 18843.817.$$

Thus, there are exactly 7 n -values for which Equation 3.5 can be satisfied in the given interval, $n = 15$ through 21. \square

The results of Section 2.4 and Figure 2.6 motivate us to make the following conjecture.

Conjecture 3.1.3. *α -values for which $g(\alpha)$ is at a local maximum represent the locations of the geometric centers of B_n .*

Thus, we can numerically solve

$$g'(\alpha) = 0 \tag{3.6}$$

near the points given by $4(14 + n)^2\pi^2$ for $n \in \{1, 2, 3, 4, 5, 6, 7\}$, to locate the centers of B_n .

Conjecture 3.1.4. *The intersection $O^+(\alpha) \cap O^+(-\alpha) \neq \emptyset$ if and only if $g(\alpha) = \alpha$.*

3.2 The Immediate Basin of Attraction

This section shows some steps we have made towards proving Conjecture 2.3.1. We use the following result (given in [4]),

Lemma 3.2.1. *If q_α is an attracting fixed point of $f(z)$ then the immediate basin of attraction of q_α contains at least one critical value of f .*

We have at least one point we know is in B_n . This is the one given by $4(14+n)^2\pi^2$, $n \in \{1, 2, \dots, 7\}$. Call this point α_n . We know it is in B_n , since it's orbit is bounded. Thus, in our image, this point would be colored black, as per Table 1.1.

Proposition 3.2.2. *$g(\alpha_n)$ lies within the basin of attraction A of the attracting fixed point of C_α .*

Proof. By Lemma 3.2.1, we know that $\alpha \in A$, and it follows that $g(\alpha_n) = \alpha \in A$. \square

REFERENCES

- [1] Devaney, R. L. *An Introduction to Chaotic Dynamical Systems*, Second Edition, 1989. Perseus Books Publishing, Reading, MA.
- [2] Durkin, M. B. *Observations on the Dynamics of the Complex Cosine-Root Family*, Journal of Difference Equations and Applications, vol. 4, 215-228, 1998.
- [3] Hallstead, M. *Dynamics of a Cosine-Root Family* , Honors Thesis, Ithaca College Department of Mathematics, 2004.
- [4] Milnor, J. *Dynamics in One Complex Variable: Third Edition* , Princeton University Press, 2006.